Different origins of acoustic streaming at resonance

Bach, Jacob Søberg; Bruus, Henrik

Published in:
Meetings on Acoustics. Proceedings

Link to article, DOI:
10.1121/2.0000927

Publication date:
2018

Document Version
Publisher's PDF, also known as Version of record

Different origins of acoustic streaming at resonance

Jacob Bach, and Henrik Bruus

Citation: Proc. Mtgs. Acoust. **34**, 022005 (2018); doi: 10.1121/2.0000927
View online: https://doi.org/10.1121/2.0000927
View Table of Contents: http://asa.scitation.org/toc/pma/34/1
Published by the Acoustical Society of America

Proceedings of Meetings on Acoustics

Volume 34 http://acousticalsociety.org/

21st International Symposium on Nonlinear Acoustics

21st ISNA

Santa Fe, New Mexico, USA July 9-13, 2018, 50th Anniversary

Computational Acoustics: Paper S25-2

Different origins of acoustic streaming at resonance

Jacob Bach and Henrik Bruus
Department of Physics, Technical University of Denmark, Kongens Lyngby, Capital Region, 2800, DENMARK; jasoba@fysik.dtu.dk; bruus@fysik.dtu.dk

Acoustic streaming is a nonlinear phenomenon that plays an essential role in microscale acoustofluidic devices for handling of sub-micrometer particles. However, the streaming patterns observed in experiments can be of complicated and non-intuitive character, and therefore, experiments, and device optimization are often carried out in a trial-and-error manner. To overcome this obstacle, we classify acoustic streaming based on our recently developed theory of acoustic streaming. Using this theory we have shown that acoustic streaming is driven partly by Reynolds stresses in the bulk and partly by a slip-velocity condition at the walls due to Reynolds stresses in the acoustic boundary layers. Hence, in our classification, we distinguish between boundary-layer-driven and bulk-driven streaming. For boundary-layer-driven streaming at resonance, we classify the two physically relevant limits of parallel and perpendicular acoustics as well as the intermediate range. For bulk-driven streaming we find that the acoustic intensity vector plays a central role, and that this quantity can give rise to a strong bulk-driven streaming, if the acoustic fields have large angular momentum. In this context, we analyze mechanisms that can lead to rotating resonant modes in acoustic microchannels.

Published by the Acoustical Society of America

 https://doi.org/10.1121/2.0000927

1. INTRODUCTION - ACOUSTIC STREAMING IN MICROCHANNELS

One of the main goals in the field of microfluidics is to scale down laboratory instruments and study microscopic biological samples precisely and efficiently. In this context, acoustofluidics offers a method to handle microparticles in a gentle and contact-free way by the use of acoustophoresis *i.e.* the migration of particles due to sound. Applications include *e.g.* size-independent sorting of cells,[1] acoustic tweezing,[2] and acoustic trapping.[3] The first central nonlinear phenomena in acoustophoresis is the acoustic radiation force which scales with the particle volume and tends to focus particles based on their acoustic contrast. The other is the rotating acoustic streaming, which tends to mix suspended particles due to the Stokes drag that scales with the particle radius. Due to these scalings, acoustic streaming is insignificant for large particles but important for small particles, where the critical particle size is around 1 μm.[4] A deep understanding of acoustic streaming is therefore important in order to control sub-micron particles using acoustophoresis.

In this work, we analyse theoretically acoustic streaming at fluid resonance, where the acoustic fluid velocity is enhanced a quality factor $Q \gg 1$ compared to velocity of the confining wall. In particular, we investigate the ill-characterized *in-plane streaming* which rotate in a plane parallel to the surrounding solid surface. Examples from the literature of such horizontal in-plane streaming patterns are the 6-by-6 flow roll-pattern observed in a 2 mm × 2 mm × 0.2 mm cavity in a silicon-glass chip shown in Fig. 4(b) of Ref. [5], and the 2-by-2 flow-roll pattern observed in a cm-long glass capillary tube with a 2 mm × 0.2 mm inner cross section in Fig. 3 of Ref. [6].

We find that this kind of streaming can be generated in closed cavities if the acoustic motion is rotating and that this rotation can be obtained spontaneously in channel geometries with small deviation from symmetry. Acoustic streaming is partly driven by a slip-boundary condition which compensates for the Reynolds stress in the narrow acoustic boundary layer of width $\delta \sim 0.5$ μm and partly by a bulk force density which arises due to viscous dissipation in the bulk. We show in relevant limits, that both of these non-linear driving mechanisms are closely related to the acoustic intensity vector.

2. THEORY OF ACOUSTIC FIELDS AND STREAMING NEAR ELASTIC SURFACES

The acoustic fields in microchannels arrise due to vibrations of the surrounding solid which is actuated externally, usually by a piezoelectric transducer. We express the instantaneous position $\boldsymbol{s}$ of the confining wall as a small harmonic displacement $\boldsymbol{s}_1(\boldsymbol{s}_0)\,\mathrm{e}^{-\mathrm{i}\omega t}$ around the equilibrium position $\boldsymbol{s}_1$,

$$\boldsymbol{s}(\boldsymbol{s}_0,t) = \boldsymbol{s}_0 + \boldsymbol{s}_1(\boldsymbol{s}_0)\,\mathrm{e}^{-\mathrm{i}\omega t}, \qquad \text{instantaneous surface position } \boldsymbol{s}. \tag{1}$$

Correspondingly, we expand the fluid pressure p and velocity $\boldsymbol{v}$ in perturbation series and relate the pressure perturbation and density perturbation through the isentropic compressibility κ_0,

$$p = p_0 + p_1(\boldsymbol{r})\mathrm{e}^{-\mathrm{i}\omega t} + p_2(\boldsymbol{r}), \qquad \boldsymbol{v} = \boldsymbol{0} + \boldsymbol{v}_1(\boldsymbol{r})\mathrm{e}^{-\mathrm{i}\omega t} + \boldsymbol{v}_2(\boldsymbol{r}), \qquad \kappa_0 = \frac{1}{\rho_0}\Big(\frac{\partial\rho}{\partial p}\Big)_S = \frac{1}{\rho_0 c_0^2}, \tag{2}$$

with equilibrium density ρ_0 and sound speed c_0. Here, superscripts indicate order of smallness in the acoustic Mach number $\mathrm{Ma} = \frac{|\boldsymbol{v}_1|}{c_0} \sim |p_1|\kappa_0$ with superscript "0" being the equilibrium value, "1" being the amplitude of the first-order linear acoustic motion and "2" referring to a second-order time-averaged quantity generated by products of first-order fields. In particular, $\boldsymbol{v}_2$ is the acoustic streaming which, away from the acoustic boundary layer of width $\delta \sim 0.5$ μm, is governed by an incompressible Stokes equation with a driving force density $\boldsymbol{f}^{\mathrm{str}}$ proportional to the time-averaged acoustic intensity vector $\langle \boldsymbol{S}_{\mathrm{ac}} \rangle = \langle p_1 \boldsymbol{v}_1 \rangle$,[7]

$$\boldsymbol{\nabla}\cdot\boldsymbol{v}_2 = 0, \qquad \boldsymbol{0} = -\boldsymbol{\nabla}\tilde{p}_2 + \eta_0\nabla^2\boldsymbol{v}_2 + \boldsymbol{f}^{\mathrm{str}}, \qquad \boldsymbol{f}^{\mathrm{str}} = \Big(\frac{4}{3}\eta_0 + \eta_0^{\mathrm{b}}\Big)\kappa_0 k_0^2 \langle \boldsymbol{S}_{\mathrm{ac}} \rangle. \tag{3}$$

where η_0 is dynamic viscosity and η_0^{b} is the bulk viscosity. To fulfil no slip at the instantaneous surface position $\boldsymbol{s}(\boldsymbol{s}_0,t)$, the streaming outside the boundary-layer must take a finite slip velocity at the wall to compensate for the inner streaming inside the boundary layer,

$$\boldsymbol{v}_2 = \boldsymbol{v}_2^{\mathrm{slip}}, \qquad \text{streaming-slip velocity at the wall equilibrium position } \boldsymbol{s}_0. \tag{4}$$

In general $\boldsymbol{v}_2^{\mathrm{slip}}$ involves complicated curvilinear derivatives of both the acoustic velocity $\boldsymbol{v}_1$ and the surface velocity $\boldsymbol{V}_1^0 = \partial_t \boldsymbol{s}$ but in the special case of fluid resonance, where the fluid velocity is enhanced a quality factor $Q \gg 1$ compared to the wall velocity, we have shown[7] that this slip-boundary condition simplifies in the two relevant limits of parallel and perpendicular acoustics,

$$\boldsymbol{v}_{2\parallel}^{\mathrm{slip}} \approx \frac{\kappa_0}{2}\big\langle \boldsymbol{S}_{\mathrm{ac}\parallel}\big\rangle - \frac{1}{2\omega\rho_0}\boldsymbol{\nabla}_\parallel\big(E_{\mathrm{kin}} - 2E_{\mathrm{pot}}\big) \quad \text{for parallel acoustics,} \qquad |\nabla_\perp^2 p_1| \ll |\nabla_\parallel^2 p_1|, \tag{5a}$$

$$\boldsymbol{v}_{2\parallel}^{\mathrm{slip}} \approx -\kappa_0\big\langle \boldsymbol{S}_{\mathrm{ac}\parallel}\big\rangle, \qquad\qquad\qquad\qquad \text{for perpendicular acoustics,} \qquad |\nabla_\perp^2 p_1| \gg |\nabla_\parallel^2 p_1|, \tag{5b}$$

with $v_{2\perp}^{\mathrm{slip}} \approx 0$ in both cases. Here $E_{\mathrm{kin}} = \frac{1}{4}\rho_0|\boldsymbol{v}_1|^2$ is the kinetic energy and $E_{\mathrm{pot}} = \frac{1}{4}\kappa_0|p_1|^2$ is the potential energy of the first order acoustic motion.

A. IN-PLANE STREAMING AND ROTATING ACOUSTICS

From Eq. (3) and Eq. (5) we see that acoustic streaming is driven partly by the bulk force density $\boldsymbol{f}^{\mathrm{str}}$ and partly by a slip condition $\boldsymbol{v}_2^{\mathrm{slip}}$. Only terms with non-zero curl can drive in-plane streaming so only $\langle \boldsymbol{S}_{\mathrm{ac}}\rangle$ is relevant if it has non-zero curl, which we find to be proportional to the acoustic angular momentum $\boldsymbol{\mathcal{L}}$,[7]

$$\boldsymbol{\nabla}\times\big\langle \boldsymbol{S}_{\mathrm{ac}}\big\rangle = \omega^2\big\langle \boldsymbol{r}_1^d\times(\rho_0\boldsymbol{v}_1^d)\big\rangle = \omega^2\boldsymbol{\mathcal{L}}, \qquad \boldsymbol{r}_1^d = \frac{\mathrm{i}}{\omega}\boldsymbol{v}_1^d. \tag{6}$$

Therefore, in-plane streaming at resonance is associated with rotating acoustics. As illustrated in Fig. 1, this rotation can be obtained if two resonances are oscillating perpendicularly with phase difference of around $\frac{\pi}{2}$. The geometry is similar to Fig. 4(b) in Ref. [5] with actuation from the bottom and a small symmetry deviation where introduced by the aspect ratio $\Delta = \frac{W_x}{W_y}$ which is slightly larger than unity.

B. IN-PLANE BULK-DRIVEN AND BOUNDARY-DRIVEN STREAMING

Bulk-driven streaming is governed by Eq. (3) and assuming $\nabla_\perp^2 \sim L_\perp^{-2}$, we can estimate the ratio of bulk-driven to boundary-driven in-plane streaming velocity from the curl of Eqs. (3) and (5),

$$\frac{|(\nabla\times\boldsymbol{v}_2^{\text{bulk-driven}})_\perp|}{|(\nabla\times\boldsymbol{v}_2^{\text{boundary-driven}})_\perp|} \propto (k_0 L_\perp)^2. \tag{7}$$

In conclusion, bulk-driven in-plane streaming will dominate for sufficiently high frequency $f = \frac{1}{2\pi}c_0k_0$ or sufficiently large height ($\sim L_\perp$), whereas boundary-driven streaming will dominate else for low frequencies and narrow channels. This point is shown in Fig. 2 where we show that $\boldsymbol{f}^{\mathrm{str}}$ increases for higher frequencies whereas $\boldsymbol{v}_2^{\mathrm{slip}}$ stays almost constant. Fig. 2(c) reproduces the experimental results of 6x6 rolls shown in Fig. 5(b) of Ref. [5] and shows that the observed streaming is bulk-driven by $\boldsymbol{f}^{\mathrm{str}}$ rather than boundary-driven by $\boldsymbol{v}_2^{\mathrm{slip}}$. Further, from Fig. 2(a) we expect that 2×2 rolls will not be clearly observable in this setup.

The investigations in Figs. 1 and 2 are examples of *parallel acoustics*. Increasing the frequency to obtain a half standing wave in the z-direction will change the situation to *perpendicular acoustics* where we should instead use the boundary condition (5b), which is always counteracting the bulk force.

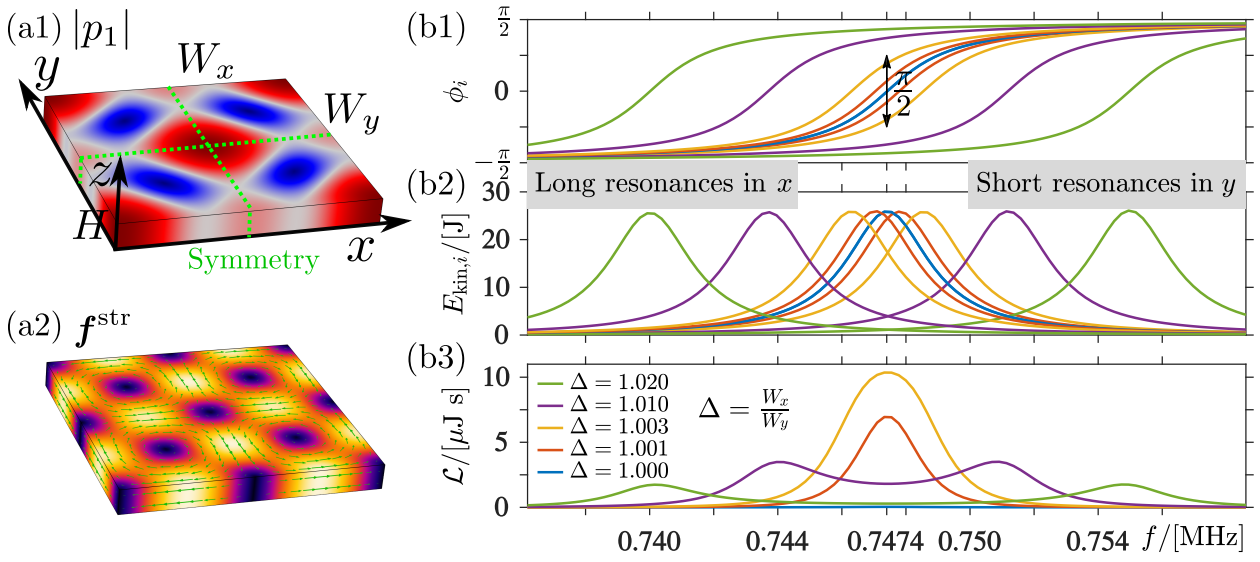

Figure 1: Simulation of rotating acoustics at resonance in a closed cavity of widths $W_x = 2000\ \mu\mathrm{m}(1 + \frac{1}{2}\Delta)$, $W_y = 2000\ \mu\mathrm{m}(1 - \frac{1}{2}\Delta)$ ***and height*** $H = 200\ \mu\mathrm{m}$ ***for small aspect ratio*** $\Delta \approx \frac{W_x}{W_y}$. ***(a1) Absolute pressure*** $|p_1|$ ***and the green symmetry lines used in Fig. 2. (a2) The generated rotating streaming force*** $\boldsymbol{f}^{\mathrm{str}}$. ***(b1) Temporal phase*** ϕ_i ***and (b1) the kinetic energy*** $E_{\mathrm{kin},i}$ ***for the long (left curves) and short resonances (right curves) for different aspect ratios. (a3) shows the resulting acoustic angular momentum*** $\mathcal{L}$.

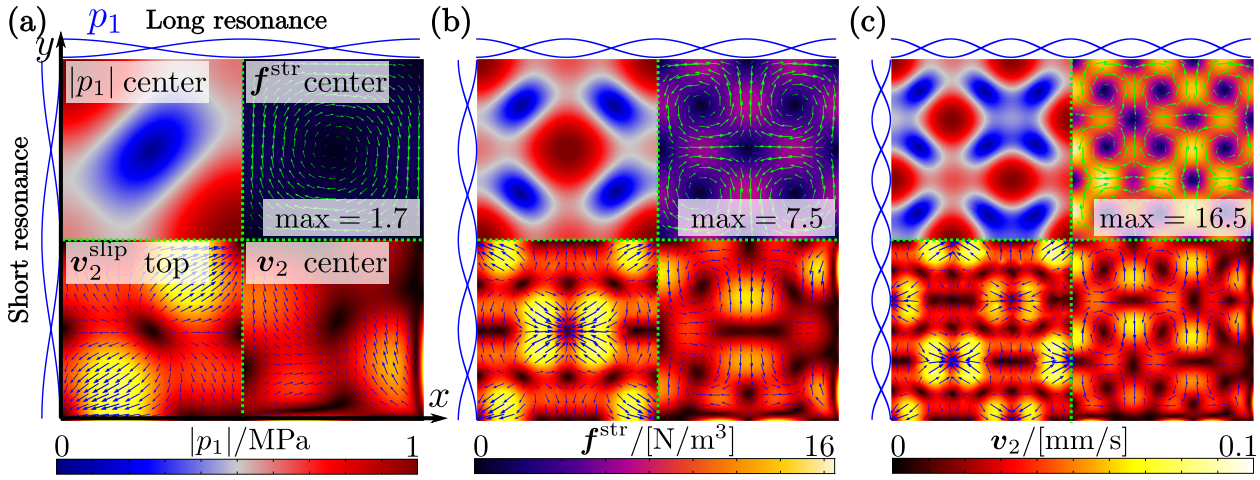

Figure 2: $|p1|$, $\boldsymbol{f}^{\mathrm{str}}$, $\boldsymbol{v}_2^{\mathrm{slip}}$ ***and*** $\boldsymbol{v}_2$ ***in the*** xy***-plane of the setup and green symmetry lines shown in Fig. 1 (a1) for three different frequencies giving 1 (a), 2 (b) and 3 (c) wavelengths in each direction respectively. Note that boundary-driven streaming generated by*** $\boldsymbol{v}_2^{\mathrm{slip}}$ ***dominates for low frequencies (a) whereas bulk-driven streaming generated by*** $\boldsymbol{f}^{\mathrm{str}}$ ***dominates for high frequencies (c).***

3. CONCLUSION AND OUTLOOK

We have presented driving mechanisms for in-plane acoustic streaming in a closed cavity and shown that this kind of streaming is associated with rotating acoustics. The two fundamental driving mechanisms are the slip velocity $\boldsymbol{v}_2^{\mathrm{slip}}$ and the bulk force density $\boldsymbol{f}^{\mathrm{str}}$, and these are both related to the acoustic intensity vector $\langle \boldsymbol{S}_{\mathrm{ac}} \rangle$. Rotating acoustics at resonance is obtained at small deviations from symmetry where two pressure modes resonate at the same frequency with a relative phase shift. We introduced the limits of parallel and perpendicular acoustics and showed that in these limits $\langle \boldsymbol{S}_{\mathrm{ac}} \rangle$ is the only physical quantity that can lead to in-plane streaming. In a setup with parallel acoustics similar to experiments[5] we found that the in-plane streaming was bulk-driven and predicted that it would not be clearly observable for lower frequencies, since the bulk force density $\boldsymbol{f}_{\mathrm{ac}}$ increases with the the frequency squared.

We are currently working on a similar characterization of acoustic streaming in long open capillaries. Here, small reflections and damping in the open direction may become important and not straight forward to model. We believe however, that the presented principle of rotating acoustics leading to in-plane streaming carries over in many different experimental setups.

REFERENCES

[1] P. Augustsson, C. Magnusson, M. Nordin, H. Lilja, and T. Laurell, "Microfluidic, label-free enrichment of prostate cancer cells in blood based on acoustophoresis", Anal. Chem. **84**(18), 7954-7962 (2012)

[2] B. W. Drinkwater,"Dynamic-field devices for the ultrasonic manipulation of microparticles", Lab Chip **16**, 2360-2375 (2016)

[3] B. Hammerström, M. Evander, J. Wahlström, and J. Nilsson, "Frequency tracking in acoustic trapping for improved performance stability and system surveillance," Lab Chip **14**, 1005-1013 (2014)

[4] P. B. Muller, R. Barnkop, M. J. H. Jensen, and H. Bruus, "A numerical study of microparticle acoustophoresis driven by acoustoc radiation forces and streaming-induced drag forces," Lab Chip **12**, 4617-4627 (2012)

[5] S. M. Hagster, T.G. Jensen, H. Bruus and J.P. Kutter, "Acoustic resonances in piezo-actuated microfluidic chips: full-image micro-PIV experiments and numerical simulations", Lab Chip **7**, 1336-1344 (2007)

[6] B. Hammarström, T. Laurell, and J. Nilsson, "Seed particle enabled acoustic trapping of bacteria and nanoparticles in continuous flow systems", Lab Chip **12**, 4296-4304 (2012)

[7] J. S. Bach and H. Bruus, "Theory of pressure acoustics with viscous boundary layers and streaming in curved elastic cavities", JASA **44**(2), 766-784 (2018)